New Results
Plant Biology

Title

Enhanced genome integrity maintenance and few directly stress-mitigating alterations in extreme habitat-adapted *Arabidopsis halleri*

Authors

Gwonjin Lee[1,a], Julia Quintana[1,§], Hassan Ahmadi[1,§], Nadežda Janina[1], Veronica Preite[1], Lara Syllwasschy[1], Justin E. Anderson[1], Björn Pietzenuk[1] and Ute Krämer[1,*]

Affiliations and Symbols

[1]Molecular Genetics and Physiology of Plants, Ruhr University Bochum, Bochum Germany

[a]Present address: Department of Botany and Plant Pathology, Purdue University, IN, USA

[§]These authors contributed equally

***Corresponding author**

Professor Dr. Ute Krämer, Molecular Genetics and Physiology of Plants, Ruhr University Bochum

Universitaetsstr. 150 ND3/30 Box 44, D-44801 Bochum, Germany

Email: Ute.Kraemer@ruhr-uni-bochum.de

ORCID: 0000-0003-2207-3975 (GL), 0000-0002-5145-3590 (JQ), 0000-0001-9354-6886 (HA), 0000-0002-0162-9340 (NJ), 0000-0002-1232-7479 (VP), 0000-0002-5388-3578 (LS), 0000-0001-7642-4641 (JEA), 0000-0002-2688-3783 (BP), 0000-0001-7870-4508 (UK)

Keywords: heavy metal, meiosis, edaphic adaptation, extremophile, Brassicaceae, metal hyperaccumulation

Author Contributions: Designed research: UK, GL, JQ, JEA, BP; conducted experiments: GL, JQ, HA, VP, LS; analyzed data: GL, UK, JQ, HA, NJ, BP, LS; wrote paper: GL, UK, with contributions from JQ, HA, BP, VP.

Abstract

Heavy metal-rich toxic soils and ordinary soils are both natural habitats of *Arabidopsis halleri*, different from closely related plant species such as *A. thaliana*. Here we demonstrate enhanced Cd hypertolerance and attenuated Cd accumulation in plants originating from the most highly heavy metal-contaminated *A. halleri* site in Europe Ponte Nossa (Noss/IT), compared to *A. halleri* from non-metalliferous (NM) sites at both a small and a larger geographic distance. In the two populations from NM sites, hundreds of Cd-responsive transcripts mostly reflect the activation of Fe deficiency responses, whereas no single transcript responded to the same Cd treatment in plants from the metalliferous (M) site Noss. Instead, in Noss, thousands of transcripts exhibited an altered abundance irrespective of Cd exposure, with the highest enrichment for Gene Ontology Term "meiotic cell cycle". Levels of *ARGONAUTE 9* (*AGO9*) and the synaptonemal complex transverse filament protein-encoding *ZYP1a/b* transcripts, which are pre-meiosis- and meiosis-specific in *A. thaliana*, respectively, were strongly elevated in vegetative tissues of Noss, alongside transcripts with known additional functions in somatic genome integrity maintenance. Increased *AGO9* transcript abundance was shared by individuals from M sites in Poland and Germany. Expression of *IRON-REGULATED TRANSPORTER 1* (*IRT1*) was very low and of *HEAVY METAL ATPASE 2* (*HMA2*) strongly elevated in Noss compared to both NM populations, largely explaining physiological differences in Cd handling. In summary, adaptation of Noss to extreme abiotic stress is associated with globally enhanced somatic genome integrity maintenance, as well as a small number of constitutive alterations in stress-specific functional networks.

Introduction

Heavy metals, such as zinc (Zn), cadmium (Cd) and lead (Pb), are naturally omnipresent in the biosphere at very low levels. Their concentrations can be regionally elevated and are extremely high locally at rare sites as a result of geological anomalies. Human activities, for example ore mining, metallurgical processing and sewage sludge deposition, contribute to anthropogenic contamination of the biosphere with heavy metals, threatening environmental and human health (Nriagu and Pacyna 1988; Lamas et al. 2016). Heavy metal-enriched habitats often host characteristic ecological communities, especially where human activities have introduced extremely high, toxic levels of heavy metals only recently after the beginning of the industrial revolution (Ernst 1974). Here we use comparative transcriptomics to uncover the molecular basis of local adaptation to a highly heavy metal-contaminated soil in a land plant as a complex multi-cellular eukaryotic organism.

The Brassicaceae species *Arabidopsis halleri*, in the sister clade of the genetic model plant *Arabidopsis thaliana*, is an emerging perennial model plant (Krämer 2015; Honjo and Kudoh 2019; Nagano et al. 2019). *A. halleri*, a stoloniferous obligate outcrosser, has repeatedly colonized highly heavy metal-contaminated, so-called metalliferous (M) soils (Ernst 1974; Bert et al. 2000; Stein et al. 2017). Natural populations of *A. halleri* are also found on non-contaminated (non-metalliferous, NM) soils. Irrespective of its habitat soil type, *A. halleri* is a Zn and Cd hyperaccumulator (Ernst 1974; Bert et al. 2000; Stein et al. 2017). The about 750 known hyperaccumulator plant species are land plants of which at least one individual was identified to accumulate a metal or metalloid in its above-ground tissues to concentrations more than one order of magnitude above critical toxicity thresholds of ordinary plants, at its natural site of growth in the field (Reeves et al. 2018). Hyperaccumulation in plants can act as an elemental defense against biotic stress, and the associated species-wide heavy metal tolerance can facilitate the colonization of M soils by *A. halleri* (Kazemi-Dinan et al. 2014).

Cross-species comparative transcriptomics studies of *A. halleri* and *A. thaliana* established tens of candidate metal homeostasis genes for roles in metal hyperaccumulation or metal hypertolerance, which encode various transmembrane transporters of metal cations and isoforms of a metal chelator biosynthetic enzyme (Becher et al. 2004; Weber et al. 2004; Talke et al. 2006). Subsequent work demonstrated functions in metal hyperaccumulation or hypertolerance for some of these genes. The key locus making the largest known contribution to both metal hyperaccumulation and hypertolerance in *A. halleri* is *Heavy Metal ATPase 4* (*HMA4*), which encodes a plasma membrane P_{1B}-type metal ATPase mediating cellular export for xylem loading of Zn and Cd in the root (Talke et al. 2006; Hanikenne et al. 2008). Transcript levels of *HMA4* are substantially higher in *A. halleri* than in *A. thaliana* independently of cultivation conditions, as was also observed for many other candidate genes. A combination of modified *cis*-regulation and gene copy number expansion

accounts for high expression of *HMA4* (Hanikenne et al. 2008). Examples of other candidate genes with experimentally demonstrated functions in *A. halleri* include *NAS2* (Deinlein et al. 2012) contributing to Zn hyperaccumulation, *MTP1* (encoding a vacuolar Zn^{2+}/H^{+} exchanger) acting in Zn tolerance (Dräger et al. 2004) and *CAX1* (Ca^{2+}/H^{+} exchanger 1) functioning to enhance Cd tolerance (Baliardini et al. 2015). While metal hyperaccumulation and hypertolerance are species-wide traits in *A. halleri*, there is additionally a large extent of within-species variation in the levels of metal accumulation, metal tolerance and gene expression (Meyer et al. 2015; Stein et al. 2017; Corso et al. 2018; Schvartzman et al. 2018).

Within-species transcriptomic differences between *A. halleri* populations originating from M and NM soils can provide insights into the molecular alterations associated with the natural colonization of M soils, but they have remained unexplored thus far. To address local adaptation to M soil in *A. halleri*, we focused here on the population at the most highly heavy metal-contaminated *A. halleri* site in Europe at Ponte Nossa (Noss/IT) according to a large field survey (Stein et al. 2017). Noss individuals were more Cd-tolerant and accumulated lower levels of Cd than both closely related *A. halleri* from a population on NM soil in the vicinity, Paisco Loveno (Pais), and more distantly related *A. halleri* from Wallenfels (Wall) on NM soil in Germany. Further contrasting with plants of NM soil origin, transcriptomic Cd responses including the activation of Fe deficiency responses were attenuated in the highly Cd-tolerant population. Instead, a large number of transcripts differed in abundance in Noss (M soil origin) from both Pais and Wall plants (NM soil origins) irrespective of cultivation conditions. Differences comprised primarily the global activation of meiosis- and genome integrity maintenance-related functions in somatic tissues of Noss, accompanied by pronouncedly altered levels of few metal homeostasis transcripts known for central roles in Cd accumulation and basal Cd tolerance of *A. thaliana*. Our results suggest the possibility of somatic functions in *A. halleri* (Noss) for some known meiosis genes. This work provides insights into how land plants cope with rapid anthropogenic environmental change and extreme abiotic stress levels.

Results

Choice of populations and comparative physiological characterization

In a field survey of 165 *Arabidopsis halleri* sites across Europe, average soil Cd concentrations were highest at Ponte Nossa/IT (Noss) in both the total and hydrochloric acid-extractable soil fractions (900 and 203 mg Cd kg^{-1} soil, respectively; second highest were 130 and 87 mg Cd kg^{-1} soil, respectively)(Stein et al. 2017). Therefore, we chose the *A. halleri* population at this M site as the focal population in this comparative study, in combination with two populations at NM sites for comparison, one near Paisco Loveno (Pais/IT) approximately 38 km northeast of Noss, and one near

Wallenfels (Wall/DE) about 520 km to the North. Average soil total Cd concentrations in close proximity of the *A. halleri* individuals studied here were 700-fold higher at Noss than at Pais (supplementary table 1, Supplementary Material online). Previously published transcriptome studies of Zn/Cd hyperaccumulator plant species included individuals originating from geographically distant M sites, but were not designed to compare between M and NM sites (Corso et al. 2018; Schvartzman et al. 2018; Halimaa et al. 2019).

In order to test for local adaptation of the Noss population to high soil Cd levels, we quantified Cd tolerance of individuals collected at each of the three sites in hydroponic culture system in a growth chamber. Based on the proportion of individuals maintaining root growth in a sequential exposure test with stepwise increasing Cd concentrations, Noss was the most tolerant (fig. 1a, supplementary table 2, supplementary fig. 1, Supplementary Material online). Following a different approach for quantifying metal tolerance (Schat and Ten Bookum 1992), mean EC_{100}, the effective Cd concentration causing 100% root growth inhibition in a given individual, was significantly higher for Noss (344 ± 98 µM Cd) than for Pais (219 ± 66 µM Cd) and Wall (221 ± 56 µM Cd) (fig. 1b).

In natural populations in the field, Cd concentrations accumulated in leaves of *A. halleri* at Noss were at least 20-fold higher than at Pais and 3-fold higher than at Wall (supplementary table 1, Supplementary Material online)(Stein et al. 2017). By contrast, Zn concentrations in leaves of field-collected individuals were similar in all three populations, despite vastly differing soil Zn levels. The leaf:soil ratio of Cd concentrations (Cd accumulation efficiency) in the field was highest in the Wall population from north of the Alps and lowest in Noss, suggesting attenuated leaf Cd accumulation at Noss compared to both Pais and Wall (fig. 1c). This is in accordance with previously described differences between geographic regions and between M and NM *A. halleri* sites (Meyer et al. 2015; Stein et al. 2017). Upon exposure to a sub-toxic concentration of 2 µM $CdSO_4$ in hydroponic culture for 16 d, Cd concentrations in roots of Noss (140 ± 74 µg Cd g^{-1} DW) were only 43% and 40% of those in Pais and Wall, respectively (fig. 1d, supplementary table 3, Supplementary Material online). Leaf Cd concentrations were also lower in Noss (160 ± 74 µg Cd g^{-1} DW) than in Wall (about 52% of Wall; $P < 0.05$), and at about 76% of those in Pais (n.s.). We additionally observed between-population differences in the accumulation of other nutrients (supplementary fig. 2, Supplementary Material online). Upon Cd exposure, Cu concentrations were higher, and Mn concentrations were lower than under control conditions in roots of Pais and Wall, but not in roots of Noss (supplementary fig. 2a and d, Supplementary Material online). Fe concentrations were higher in roots of Noss and increased further under exposure to Cd, in contrast to the two populations from NM soils (supplementary fig. 2e, Supplementary Material online). In shoots of Noss, Fe concentrations were about twice as high (*ca.* 75 µg Fe g^{-1} DW) than in the shoots of the other two populations under both control and Cd exposure conditions (supplementary fig. 2e, Supplementary Material online). Taken

together, these results showed that the Noss population of *A. halleri* is more tolerant to Cd than both Pais and Wall, supporting adaptation to local soil. This was associated with attenuated Cd accumulation and a distinct profile of tissue concentrations of micronutrient metals in Noss under standardized growth conditions in hydroponic culture.

Comparative transcriptomics

Transcriptome sequencing was carried out for a total of 72 samples, with three independent repeats of each experiment comprising root and shoot tissues of two genotypes from each of the three populations grown in control and Cd-amended medium for 16 d (0 and 2 µM $CdSO_4$; supplementary table 4, Supplementary Material online). Principal component analysis (PCA) suggested predominant differences between root and shoot transcriptomes (supplementary fig. 3a, Supplementary Material online). In both roots and shoots, transcriptomes of the geographically neighboring populations Noss and Pais grouped closer together in the first principal component by comparison to the geographically distant Wall population (supplementary fig. 3b, c, Supplementary Material online). This suggested that individuals from Noss and Pais are genetically more closely related to one another than either of these to individuals from Wall.

Upon long-term exposure to a low level of Cd as applied here, transcriptomic differences compared to controls comprised a few hundred genes in both the Pais and Wall populations originating from NM sites (fig. 2a and b, supplementary fig. 4, supplementary fig. 5, Supplementary Material online, Data Set 1). By contrast, in the more Cd-tolerant population Noss, no single transcript responded in abundance to Cd exposure under these conditions in either roots or shoots. To identify candidate transcripts that may contribute to the ability of the Noss population to persist on extremely highly heavy metal-contaminated soil, we thus examined the genes showing differential expression between populations (fig. 2c and d, Data Set 2). As an initial set of candidate genes, we focused on those transcripts showing differential abundance between Noss (M) and both of the populations from NM soils, Pais and Wall. This comparison identified differential transcript levels for 1,617 genes (801/599/217, higher in Noss/ lower in Noss / intermediate in Noss) in roots and 1,638 genes (797/604/237) in shoots under control conditions (under Cd exposure 848/697/236 and 1140/707/339 in roots and shoots, respectively) (surrounded by a red line in fig. 2c and d).

Candidate genes differentially expressed in Noss

We subjected the genes expressed either at higher or lower levels in Noss compared to both Pais and Wall (DEGs; 0 µM Cd; Data Set 3) to a Gene Ontology Term (GO) enrichment analysis (Data Set

4). Meiotic cell cycle (GO:0051321) was enriched in the group of genes that are more highly expressed in both root and shoot of Noss (fig. 3a, b, supplementary table 5, Supplementary Material online). Among the genes within the GO term meiotic cell cycle, transcript levels of *ARGONAUTE 9* (*AGO9*) were substantially higher in both root and shoot tissues of the Noss in comparison to both the Pais and Wall populations (fig. 3c, d, supplementary table 6, Supplementary Material online; Log_2FC = 6.6 and 4.4 to 4.6 in root and shoot, respectively; see Data Set 2). By contrast, present knowledge suggests that the expression of *AGO9* in *A. thaliana* is restricted to only a few cells during the early stages of meiotic megaspore formation (Duran-Figueroa and Vielle-Calzada 2010; Olmedo-Monfil et al. 2010). Amino acid sequence alignment of AGO proteins in *A. halleri* and *A. thaliana* (supplementary fig. 6, Supplementary Material online) confirmed that *Ah*AGO9 is the closest *A. halleri* homologue of *At*AGO9 in clade 3 of ARGONAUTE proteins (AGO4, -6, -8 and -9)(Vaucheret 2008). Sequence read coverage for *AGO9*, obtained from gDNA of Noss and Pais, suggested that *AGO9* is a single-copy gene (supplementary table 7, Supplementary Material online). In the GO class meiotic cell cycle, transcript levels of the two gene copies of *ZIPper I* (*ZYP1a* and *ZYP1b*) were also substantially higher in Noss than in both Pais and Wall (fig. 3e-f, Tables S5 and S6). Amino acid sequences of *At*ZYP1a and b are highly similar and conserved in *Ah*ZYP1a and b (supplementary fig. 7, Supplementary Material online). We validated sequencing-based transcriptomic data by reverse-transcription quantitative real-time PCR for a representative set of genes including *AGO9* and *ZYP1A/B* (supplementary table 9, supplementary fig. 9, Supplementary Material online). An additional 15 genes in roots and 10 genes in shoots of the GO meiotic cell cycle showed mildly elevated transcript levels in Noss compared to both populations of NM soil (see fig. 3a and b, Data Set 4). The partly overlapping categories homologous recombination (GO:0035825), reciprocal meiotic recombination (GO:0007131), meiosis I cell cycle process (GO:0061982) and condensed chromosome (GO:0000793) were also enriched among transcripts of increased abundance in roots of Noss. Among 23 genes over-represented in GO terms associated with meiotic cell cycle and homologous/meiotic recombination, homologs of eight genes were shown to have roles or implicated in somatic DNA repair in *A. thaliana* (supplementary table 5, Supplementary Material online). Furthermore, sulfur compound metabolic process (GO:0006790), glucosinolate biosynthetic process (GO:0019761) and plastid (GO:0009536) were enriched among transcripts of decreased abundance in shoot tissues of Noss (see Data Set 4).

Differential abundance of metal homeostasis-related transcripts between populations

Next, we sought to identify metal homeostasis candidate genes contributing to the observed differences in Cd tolerance and accumulation between Noss and the two other populations. For this

purpose, we intersected a manually curated list of metal homeostasis genes with the list of candidate transcripts (see fig. 2e-g, $|Log_2FC| > 1$, mean normalized counts across all samples > 2; Data Set 3, supplementary table 8, Supplementary Material online). Transcript levels of *Heavy Metal ATPase 2* (*HMA2*) and two *ZRT/IRT-like Protein* genes, *ZIP2* and *ZIP6*, were higher in roots of Noss than Pais and Wall (fig. 3e). Root transcript levels of *Iron-Regulated Transporter 1* (*IRT1*), *Plant Cadmium Resistance 9* (*PCR9*) and *ZIP10* were lower in Noss (fig. 3f). In shoots of Noss, transcript levels of *PCR8*, *HMA2* and *Cation/H*$^+$ *Exchanger 2* (*CHX2*) were higher than in both Pais and Wall (fig. 3g). The IRT1 transmembrane transport protein is known as the high-affinity root iron (Fe^{2+}) uptake system of dicotyledonous plants as well as the predominating path for inadvertent uptake of Cd^{2+} in Arabidopsis (Vert et al. 2002). Compared to Pais and Wall, an 84% to 92% lower expression of *IRT1* in Noss (see fig. 3f) would provide an intuitive adaptive route towards plant Cd tolerance *via* exclusion (see fig. 1d, supplementary fig. 8, Supplementary Material online). In *A. thaliana*, *IRT1* expression is under complex regulation at both the transcriptional and post-transcriptional levels (Kerkeb et al. 2008). To test whether reduced IRT1 protein levels accompany low *IRT1* transcript abundance in Noss, we carried out immunoblot detection using an anti-*At*IRT1 antibody in subsamples of root tissues from the same experiments. At the size corresponding to IRT1 of Fe-deficient *A. thaliana*, we observed weak bands in both Pais and Wall, but no band was visible in Noss, under our control and 2 µCd exposure conditions. Instead, we observed weak signals at higher apparent molecular masses, consistent with expectations for various ubiquitinated forms of IRT1, respectively (fig. 3h)(Barberon et al. 2011; Callis 2014). In *A. thaliana*, the ubiquitination of IRT1 leads to its deactivation by removal from the plasma membrane through endocytosis (Barberon et al. 2011). Taking these data together, IRT1 immunoblots were in agreement with the between-population differences observed for *IRT1* transcript levels using RNA-seq and RT-qPCR.

Cd exposure elicits transcriptional Fe deficiency responses in both populations from NM sites

Upon exposure to Cd, we found differential transcript abundance for 210 genes (upregulated 53, downregulated 157) in shoots and of 428 genes (upregulated 143, downregulated 285) in roots of Pais. A similar number of 197 (upregulated 65, downregulated 132) in roots and 243 (upregulated 98, downregulated 145) in shoots responded to Cd in Wall (see fig. 2a and b, Data Set 5). Of these, the responses of 44 genes in roots and of 84 genes in shoots were shared between both populations from NM soil, a larger number than expected by chance ($P < 10^{-50}$, hypergeometric test). Transcriptomic Cd responses of both Pais and Wall were enriched in Fe deficiency responses (fig. 4, Data Set 6). The associated enriched GO categories included cellular response to iron ion starvation (GO:0010106) among the upregulated transcripts, as well as intracellular sequestering of iron ion

(GO:0006880) and ferroxidase activity (GO:0004322) among the downregulated transcripts in both roots and shoots.

Among transcripts known to increase in abundance in *A. thaliana* under iron deficiency, transcript levels of *Popeye* (*PYE*), *Basic Helix-Loop-Helix 38/39/100/101* (*bHLH38/39/100/101*) transcription factors, *Brutus* (*BTS*) and *Brutus-like 1* (*BTSL1*), as well as *Ferric Reduction Oxidases* (*FRO1* and *FRO3*), *Nicotianamine Synthase 4* (*NAS4*), *Zinc Induced Facilitator 1* (*ZIF1*), *Oligopeptide Transporter 3* (*OPT3*) and *Natural Resistance-Associated Macrophage Protein 3* (*NRAMP3*) increased under Cd exposure (supplementary table 10a, Supplementary Material online). A number of genes have roles in iron storage/sequestration, and their transcript levels are downregulated under iron deficiency in *A. thaliana*. Of these, *Ferritin* (*FER1*, *FER3* and *FER4*) and *Vacuolar iron Transporter-Like protein* (*VTL1* and *VTL5*) transcript levels were downregulated in Cd-exposed Pais and Wall plants (supplementary table 10b, Supplementary Material online).

Further GOs enriched among transcripts downregulated in abundance in response to Cd were response to reactive oxygen species (GO:0000302), photosynthesis (GO:0015979), and chloroplast thylakoid membrane (GO:0009535). The gene content of these, however, is less compelling in implicating the respective biological processes (see supplementary table 10b, Supplementary Material online; Datasets S5 and S6). Chloroplast thylakoid membrane is a child term of plastid (GO:0009536), which was enriched among transcripts present at lower levels in Noss than in both Pais and Wall. Six genes were in common between these (supplementary table 11, Supplementary Material online), of which one, *Light Harvesting Complex of photosystem II* (*LHCB4.2*), appears to function directly in photosynthesis. A more extensive search for transcripts that are Cd-responsive in both Pais and Wall as well as differentially expressed in the Noss population identified *Bifunctional inhibitor/lipid-transfer protein/seed storage 2S albumin superfamily protein* in the root and *NAD(P)-binding Rossmann-fold superfamily protein* in the shoot (supplementary table 12, Supplementary Material online). Finally, metal homeostasis protein-encoding transcripts upregulated in abundance upon Cd exposure in Pais or Wall were generally less abundant in Noss regardless of Cd treatment (supplementary fig. 10, Supplementary Material online, cluster R5 and S5). Conversely, metal homeostasis protein-coding transcripts that were decreased in abundance under Cd exposure in Pais or Wall were generally present at higher levels in Noss (supplementary fig. 10, Supplementary Material online, cluster R2 and S2). These between-population differences primarily comprised genes associated with Fe deficiency responses of *A. thaliana* as described above (see fig. 4, supplementary table 10, Supplementary Material online), thus indicating against a constitutive proactive activation in Noss of the transcriptional Cd responses observed here in the Pais and Wall populations.

Elevated *AGO9* expression and lower transcript levels of long terminal repeat retrotransposons in Noss

Comparative transcriptomics suggested that in particular, *AGO9* transcript levels were higher in Noss compared to both Pais and Wall (see fig. 3c and d). If this were indeed the case, then we would expect that long terminal repeat retrotransposons (LTR-TEs), target loci known to be transcriptionally silenced dependent on *AGO9* in *A. thaliana*, are less transcriptionally active in *A. halleri* from Noss than *A. halleri* from Pais and Wall (Duran-Figueroa and Vielle-Calzada 2010). In Noss, transcript levels derived from LTR-TEs were lower in shoot tissues by comparison to both Pais and Wall and also lower in root tissues than in Pais (fig. 5, supplementary fig. 11, Supplementary Material online, Data Set 7).

Elevated *AGO9* transcript levels in *A. halleri* originating from European M sites

We identified two additional pairs of one *A. halleri* population at a highly metal-contaminated (M) site and one at a non-contaminated (NM) site in a common geographic region, respectively (Stein et al. 2017). Individuals originating from these sites were cultivated hydroponically alongside the individuals of this study. Quantification of *AGO9* transcript levels by RT-qPCR independently confirmed higher transcript levels in *A. halleri* individuals from Noss compared to Pais (fig. 6; see fig. 3d, Data Set 2). Moreover, *AGO9* transcript levels were higher in *A. halleri* individuals from Polish and German M sites, Miasteczko Śląskie (Mias/PL) and Lautenthal (Laut/DE), compared to their respective NM site counterparts, Zakopane (Zapa/PL) and Wallenfels (Wall/DE). This finding suggests that elevated expression of *AGO9* is common among individuals from M populations compared to their NM neighbours in several regions of Europe.

Discussion

Divergent transcript levels between populations arise more abundantly than divergent transcriptomic responses to Cd

To identify the molecular alterations associated with plant adaptation to extreme abiotic stress, we conducted comparative transcriptomics of *A. halleri* populations from contrasting environments of origin across both a small and a larger geographic distance (fig. 2; apparently reflected in a phylogenetic distance, see supplementary fig. 3 and 11, Supplementary Material online). In line with their origin from the most highly Cd-contaminated *A. halleri* site known in Europe, our data

supported environment-dependent phenotypic differentiation in *A. halleri* and adaptation to high soil Cd levels at Noss (fig. 1). Transcript levels of a few hundred genes differed between Cd-exposed and unexposed *A. halleri* plants from the two populations originating from NM soils, Pais and Wall. Thus, these plants attained a different transcriptomic state in the presence of Cd through a process that must involve the initial interaction of Cd^{2+} with primary Cd-sensing or -sensitive sites, of which the molecular identities are yet unknown. By contrast, in *A. halleri* from the Noss (M) population, there was no single gene of which transcript levels differed between the 2-µM $CdSO_4$ and the control treatment (fig. 2). This implies that in Noss, Cd^{2+} was either effectively kept away from all Cd-sensing and -sensitive sites, or Cd^{2+} did not result in any transcriptomic adjustment within a timeframe relevant for our harvest after 16 d of exposure. Given that Noss is more Cd-tolerant than both Pais and Wall (see fig. 1), the molecular mechanisms conferring tolerance must then either be active also in the absence of Cd, or alternatively their implementation operates downstream of transcript levels, for example at the translational or post-translational level.

Several thousand transcripts differed in abundance between the Noss (M) population of *A. halleri* and either one of the two populations originating from NM sites irrespective of Cd exposure (fig. 2; see also supplementary fig. 10, Supplementary Material online). This suggests that between-population transcriptomic divergence is substantial even among geographically proximal and phylogenetically more closely related *A. halleri* populations Noss and Pais (Figs. S3, S11; Anderson *et al*., manuscript in preparation), by comparison to between-population differences in responses to Cd exposure. Similarly, earlier cross-species comparative transcriptomics studies identified responses to metal exposure in *A. thaliana*, a species with only basal metal tolerance, whereas there were no remarkable additional species-specific responses among metal homeostasis genes in the metal-hypertolerant species *A. halleri* (Talke et al. 2006; Weber et al. 2006). Instead, tens of genes with predicted roles in metal homeostasis were more highly expressed in *A. halleri* compared to *A. thaliana* irrespective of the growth conditions.

Constitutive activation of meiosis-related genes and large alterations in few metal homeostasis functions in *A. halleri* from Noss

Meiosis is essential for sexual reproduction in eukaryotes and consists of a series of two consecutive cell divisions generating four haploid daughter cells that are genetically unequal among one another and compared to the mother cell (Mercier et al. 2015). Recombination takes place during the first meiotic cell division (meiosis I) through the formation of DNA double-strand breaks followed by homologous recombination between homologous chromosomes paired in the synaptonemal complex.

In seed plants, meiosis occurs exclusively in male and female gametophyte precursor cells during the reproductive phase of the life cycle. Yet, in somatic tissues we observed an overrepresentation of the Gene Ontology Term (GO) "meiotic cell cycle" among transcripts of higher abundance in Noss by comparison to both Pais and Wall (fig. 3, supplementary table 5, Supplementary Material online, Data Set 4). This included genes functioning during entry into meiosis (*AGO9*, *SWI1*), cohesion complex (*SMC3*), synaptonemal complex (*ZYP1a/b*), recombination and its control (*PRD3*, *BRCA2B*, *MHF2*, *MSH5*, *FLIP*), for example (Mercier et al. 2015). In addition to its role during meiosis, DNA double-strand break repair (DSBR) through homologous recombination (HR) functions to maintain genome integrity following DNA damage in somatic cells (Schuermann et al. 2005). Exposure of plants to an excess of aluminum, boron or heavy metal ions can cause DNA damage (Kovalchuk et al. 2001; Rounds and Larsen 2008; Sakamoto et al. 2011; Morales et al. 2016). Of the meiosis-related genes identified here, there is evidence for an additional involvement in somatic HR-mediated DSBR for *BRCA2* (Seeliger et al. 2012), *EME1A/B* (Geuting et al. 2009), *HEB2* (Sakamoto et al. 2011), *FLIP* (Bouyer et al. 2018; Fernandes et al. 2018), *RPA2B* (Liu et al. 2017) and *ERCC1* (Dubest et al. 2004) in *A. thaliana* (supplementary table 5, Supplementary Material online; Data Set 4). *ERCC1* was also implicated in non-HR nucleotide excision repair (Hefner et al. 2003).

The two most strongly differentially expressed meiosis-related genes, *AGO9* and *ZYP1a/b*, are thought to function exclusively in reproductive development of *A. thaliana*. *AGO9* is required pre-meiotically to prevent the formation of excessive gametophytic precursor cells in *A. thaliana* (Olmedo-Monfil et al. 2010). It is expressed in a single layer of somatic companion cells surrounding the megaspore mother cell, as well as in pollen. *At*AGO9 was proposed to act in the silencing of pericentromeric TEs, predominantly long terminal repeat retrotransposons (LTR-TEs), in the ovule through the interaction with 24-nucleotide small RNAs (Duran-Figueroa and Vielle-Calzada 2010). Like other organisms, plants generally inactivate TEs in order to maintain genomic stability. Exposure to abiotic stress, including also heavy metal exposure, can result in the expression and transposition of some TEs, especially LTR-TEs, in plants (Grandbastien 2015) and other organisms (Horvath et al. 2017). In *A. halleri* from Noss elevated expression of *AGO9* in somatic cells may counteract LTR-TE activation as an adaptation to their high-stress natural environment. Consistent with this hypothesis, transcripts derived from LTR-TEs were present at overall lower levels in both root and shoot tissues of Noss compared to Pais (fig. 5). We detected no increase in the levels of transcripts derived from LTR-TEs or any other TEs at 2 µM Cd compared to control conditions. It is possible that an increase in TE expression occurs at different times after the onset of Cd exposure, at higher levels of Cd exposure which plants might encounter at the Noss site at least temporarily (Krämer 2018), or in response to other abiotic stresses or combined stress exposure, in nature (see

supplementary table 1, Supplementary Material online). Published circumstantial evidence implicated *AGO9* in DNA damage repair in seedlings of *A. thaliana* (Oliver et al. 2014). Future work will address the biological functions of *AGO9* in somatic tissues of *A. halleri*. *AGO9* is unlikely to directly affect parameters that are commonly measured for quantifying metal tolerance in plants (see fig. 1). Existing antibodies against *A. thaliana* AGO9 and ZYP1 did not detect specific bands in immunoblots of *A. thaliana* floral buds or any *A. halleri* tissues in our hands (data not shown).

We propose that our results reflect a constitutive transcriptional activation of genome integrity maintenance as a component of extreme abiotic stress adaptation of *A. halleri* at Noss. The genes newly implicated here in somatic genome integrity maintenance (supplementary table 5, Supplementary Material online) may have remained unidentified in the past because their functions are specific to *A. halleri* or because very low expression levels may be sufficient to accomplish a possible somatic DNA repair function in *A. thaliana*. Cd is not the only abiotic stress factor at the Noss site in the field. Soil adjacent to the roots of *A. halleri* plants at Noss contained maximum levels also of Zn, total and extractable Pb (32,900 and 7,010 µg g^{-1}, respectively) and Cu (7,110 and 1,630 µg g^{-1}, respectively) out of 165 European sites hosting natural populations of *A. halleri* (Pais/NM: see supplementary table 1, Supplementary Material online, 73.1 and 4.93 µg Pb g^{-1} soil as well as 22.5 and 0.757 µg Cu g^{-1} soil, total and extractable, respectively)(Stein et al. 2017). Moreover, Noss is located at the southern edge of the distribution range of *A. halleri*, which may render light/UV, drought or high temperature stress, known to prevail on bare M sites, even more relevant abiotic environmental factors (Spampinato 2017).

Attenuated Cd accumulation in *A. halleri* from Noss (see fig. 1) observed here in hydroponics is consistent with earlier results from the cultivation of Noss and Wall on an artificially Cd-contaminated soil (Stein et al. 2017) and with observations in hydroponic culture on accessions collected nearby (Meyer et al. 2015; Corso et al. 2018). Among metal homeostasis genes, we observed substantially reduced *IRT1* expression in roots of Noss compared to both Pais and Wall at both the transcript (fig. 3f) and protein level of the transport-active form (fig. 3h). This can account for both enhanced Cd hypertolerance and attenuated Cd accumulation in *A. halleri* from Noss when extrapolating from *A. thaliana irt1* mutants (Vert et al. 2002). Taking our data together, comparably high tissue levels of iron (supplementary fig. 1, Supplementary Material online) in Noss plants appear to arise independently of IRT1 (fig. 3h), which warrants further study.

Distinctly higher transcript levels of *HMA2* in both roots and shoots of Noss (fig. 3e, g) when compared to both the Pais and the Wall populations suggest that enhanced cellular export of Cd contributes to enhanced Cd hypertolerance in this population. Alongside HMA4, the plasma membrane efflux pump HMA2 mediates root-to-shoot translocation of Zn in *A. thaliana* and can also

transport chemically similar Cd^{2+} ions (Hussain et al. 2004). *HMA2* transcript levels are present in roots of Zn-deficient *A. thaliana*, in particular (Sinclair et al. 2018). To further address a possible role of *HMA2* in the adaptation of *A. halleri* to local soil composition, localization of the cell types expressing *HMA2*, as well as genetic approaches, will be required.

Cd exposure induces Fe deficiency responses in both populations from NM sites

In the Wall and Pais populations from NM soils, we observed Fe deficiency response-like transcriptomic changes upon exposure to 2 µM Cd for 16 d (fig. 4; supplementary table 10, Supplementary Material online). Plants that are non-hypertolerant to metals, for example *A. thaliana*, activate aspects of Fe deficiency responses when exposed to an excess of heavy metals, for example Cd (Leskova et al. 2017). Consequently, our observation may be seen as unsurprising. However, previously published results in *A. thaliana* were from heavy metal treatment conditions causing a mix of possible toxicity symptoms and acclimatization responses. By contrast, in this present study the Cd treatment condition was far below toxicity thresholds of *A. halleri* that is known for species-wide Cd hypertolerance (see fig. 1). Our data suggest that even under exposure to very low sub-toxic Cd concentrations, transcriptional responses of *A. halleri* reflect symptoms of nutrient imbalances caused by Cd and accomplish a compensatory role in acclimatization at the same time.

Transcriptomics studies reported Fe deficiency responses in *A. halleri* from the PL22 (M) population, but not in the I16 (M) population from close to Noss (M), in response to high-Zn exposure (Schvartzman et al. 2018). Moreover, a highly Cd-hyperaccumulating accession of *Noccaea caerulescens* exhibited a Cd-induced Fe deficiency response, by contrast to a low Cd-accumulating accession (Halimaa et al. 2019). Both of these earlier studies were lacking the comparison with a population from an NM soil environment likely to reflect the most recent environment in evolutionary history, different from the work presented here. Consequently, central aspects of the observed metal responses relating to Fe acquisition systems and tissue Fe contents are different in the comparisons of this study (supplementary fig. 1, supplementary table 10, Supplementary Material online).

What enables *A. halleri* plants to colonize toxic soils?

The conserved steady-state hypothesis postulates that plant adaptations to toxic levels of heavy metals in soil entail both attenuated cellular metal uptake and the balancing of elevated rates of inadvertent metal influx through constitutively elevated rates of sequestration away from internal cellular metal-sensing/-sensitive sites (Krämer 2018). This present work implicates alterations in the

expression of *IRT1* and *HMA2*, respectively, in these processes in Noss, an *A. halleri* population on a soil that is exceptionally rich in Cd. The conserved steady-state hypothesis also postulates that these processes operate constitutively in plants at rates adjusted to the local metal levels in the soil of origin to maintain internally available cellular metal at identical levels in contrasting natural habitats. This could explain the transcriptional responses to Cd-induced nutrient imbalance in Pais and Wall, and their absence in Noss in this study. In an extreme environment, quantitatively larger spatial and temporal variation in the respective stress factor require enhanced capabilities for the protection from and repair of cellular damage (Krämer 2018). Our study implicates enhanced genome integrity maintenance in plant adaptation to extreme stress, with contributions of hitherto unsuspected gene functions.

There is some genetic evidence that M sites were colonized independently by *A. halleri* from NM sites in the geographic vicinity (Pauwels et al. 2005; Pauwels et al. 2012). Based on only a small number of genome scans conducted so far, researchers concluded that distinct colonization events mostly involved differing genetic loci, with only little evidence for convergence (Meyer et al. 2009; Preite et al. 2019). Integrating published conclusions (Corso et al. 2018; Schvartzman et al. 2018) with the results from this differently designed transcriptomics study, it appears that the colonization of M sites in Italy and Poland was associated with expression changes of differing genes of the metal homeostasis network. In contrast, here we show that enhanced transcript levels of *AGO9* are shared among populations at M sites in distinct geographic regions, which correspond to independent colonization events (fig. 6). So why has *AGO9* not been identified in genome scans for signatures of selection (Preite et al. 2019)? We expect signatures of selection at yet unidentified loci governing *AGO9* transcript levels in *trans* (see fig. 6). Indeed, these may have been identified but cannot presently be linked with *AGO9*. Alternatively, signatures of selection are expected within non-coding regions in *cis* of *AGO9*. In genome scans, false negatives can arise from a variety of causes and are more likely to affect non-coding regions. Moreover, in the genome scans conducted in both *A. halleri* and *A. arenosa* to date, sequence reads were mapped to the reference genome of a different species, *A. lyrata*, (Yant et al. 2013; Arnold et al. 2016; Preite et al. 2019). This will result in missing data for non-conserved regions of the *A. halleri* genome, comprising non-coding regions and species-specific genes, in particular. Genome scans have addressed the molecular basis of plant adaptation to ultramafic/serpentine soils, which are Ni and Mg-rich among other mineral imbalances (Turner et al. 2010; Arnold et al. 2016). These studies identified an overlapping set of candidate genes in *A. lyrata* and *A. arenosa* which encode orthologues mostly of membrane proteins of *A. thaliana* with known or predicted roles in Mg, Ca, K, Ni, Fe and N transport. Introgression from *A. lyrata* was proposed as the origin of serpentine alleles in *A. arenosa* (Arnold et al. 2016). The biological functions of the

identified loci and sequence variants on serpentine soils remain to be addressed. Recent comparative transcriptomics studies identified sets of genes with different overlapping orthologues in *A. thaliana* as more highly expressed in Ni hyperaccumulators on serpentine soil than in closely related non-accumulator plants on other soils (de la Torre et al. 2018; Meier et al. 2018; van der Pas and Ingle 2019). Several DNA integrity maintenance genes were found to be more highly expressed in serpentine than in non-serpentine accessions of *Senecio coronatus*, but no quantitative enrichment was reported (Meier et al. 2018). It must be noted that the plants compared contrast not only in their edaphic habitat, but also in the metal hyperaccumulation trait, different from *A. halleri* populations Noss and Pais of this study.

In summary, our comparative study of *A. halleri* populations from different soil types of origin identifies transcriptomic alterations in plants adapted to an extreme environment, highly heavy metal-contaminated soil that has arisen through rapid anthropogenic environmental change.

Materials and Methods

Plant material and growth conditions

Cuttings were made of *A. halleri* ssp. *halleri* O'Kane & Al-Shehbaz individuals originating from the field (Stein et al. 2017), followed by hydroponic pre-cultivation for 4 weeks to obtain rooted vegetative clones. Experiments were conducted in 1x modified Hoagland's solution (Becher et al. 2004) with weekly exchange of solutions. In Cd tolerance assays, plants were sequentially exposed to step-wise increasing concentrations of $CdSO_4$ (0, 25, 50, 75, 100, 125, 150, 175, 200, 250, 300, 350, 400 and 450 µM) once per week in a growth chamber (10-h light at 90 µmol photons m^{-2} s^{-1}, 22°C/ 14-h dark at 18°C, 65% constant relative humidity). Cd tolerance index was quantified as EC_{100}, the effective Cd concentration causing 100% root growth inhibition (Schat and Ten Bookum 1992). For transcriptome sequencing and multi-element analysis (supplementary table 4, Supplementary Material online), 1x modified Hoagland's solution was supplemented with either 2 or 0 (control) µM $CdSO_4$, with cultivation in 16-h light (90 µmol photons m^{-2} s^{-1}, 22°C)/ 8-h dark (18°C) cycles at 60% constant relative humidity for 16 d.

Multi-element analysis and transcriptome sequencing

For multi-element analysis, apoplastically bound metal cations were desorbed from freshly harvested roots (Cailliatte et al. 2010). All tissues were washed twice in ddH_2O before drying, digestion and multi-element analysis as described (Stein et al. 2017). For transcriptome sequencing, root and shoot tissues were harvested separately 7 h after the onset of the light period, frozen immediately in liquid

nitrogen, pooled from six replicate clones per genotype, treatment and experiment, and stored at -80°C. Total RNA was extracted from aliquots of tissue homogenates using the RNeasy Plant Mini Kit (Qiagen, Hilden, Germany). One µg of total RNA was used in NEBNext Ultra II RNA Library Prep Kit for Illumina (New England Biolabs, Frankfurt, Germany), followed by sequencing to obtain 14 to 29 mio. 150-bp read pairs per sample that passed quality filters (Novogene, Hongkong).

Sequence data analysis

Reads were mapped to the *A. halleri* ssp. *gemmifera* (Matsumura) O'Kane & Al-Shehbaz accession Tada mine (W302) reference genome (Briskine et al. 2017) using HISAT2 version 2.1.0 (Kim et al. 2015). This reference genome contains a more complete set of *A. halleri* coding regions than the *A. lyrata* reference genome, and its use resulted in considerably higher mapping rates. After multiple mapping error correction according to COMEX 2.1 (Pietzenuk et al. 2016), the number of fragments per gene were determined using Qualimap2 (Okonechnikov et al. 2016), followed by principal component analysis (PCA) and differential gene expression analysis using the R package *DESeq2* (Love et al. 2014). Clustering was performed using the R package *pheatmap*. For gene ontology (GO) term enrichment analyses *A. halleri* gene IDs were converted into *A. thaliana* TAIR10 AGI codes, which were then used in hypergeometric distribution estimation through the function g:GOSt built in g:Profiler (Reimand et al. 2016). TE transcript levels were quantified based on Reads Per Kilobase per Million reads (Mortazavi et al. 2008) after mapping to the *Arabidopsis lyrata* MN47 reference genome with TE annotations (Pietzenuk et al. 2016). This was necessary because the *A. halleri* ssp. *gemmifera* reference genome lacks contiguity outside coding sequences and in repetitive regions and its TE annotations are less thoroughly curated. Reads were used to reconstruct cDNA variants with Integrated Genome Viewer (Robinson et al. 2017). Multiple comparisons of means were conducted using the *stats* and *agricolae*, with normality and homoscedasticity tests in the *car*, packages in R (R_Core_Team 2013).

Validation by RT-qPCR and immunoblots

We used aliquots of homogenized tissues as frozen during harvest. Real-time RT-qPCR reactions were run in a 384-well LightCycler®480 II System (Roche Diagnostics, Mannheim, Germany) using the GoTaq qPCR Mastermix (Promega, Walldorf, Germany) and cDNAs synthesized from DNase-treated total RNA using the RevertAid First Strand cDNA Synthesis Kit (Thermo Fisher Scientific, Schwerte, Germany). Immunoblots were carried out following SDS-PAGE (Lämmli 1970) using anti-*At*IRT1 (AS11 1780, Lot number 1203; Agrisera, Vännas, Sweden), HRP-conjugated secondary antibodies (Thermo Fisher Scientific) and detection using the ECL Select Western Blotting Detection Reagent (GE Healthcare, Little Chalfont, England) and a Fusion Fx7 GelDoc (Vilber Lourmat, Eberhardzell, Germany).

Acknowledgements

We are grateful to Raphael Mercier (Max Planck Institute for Plant Breeding Research, Cologne, Germany) and Jean-Philippe Vielle-Calzada (CINVESTAV, Mexico City, Mexico) for materials. We thank Petra Düchting, Andreas Aufermann and Jan Riering for assistance (Ruhr University Bochum, Germany). This work was supported by the Deutsche Forschungsgemeinschaft (Research Priority Program SPP1529 ADAPTOMICS, start-up grant to GL/JEA from grant number Kr1967/12 to UK, Research Priority Program SPP1819 RAPID EVOLUTION grant number Kr1967/16 to UK, and individual grant (Kr1967/3-3 to UK); and European Research Council Advanced Grant (grant number 788380 to UK). We acknowledge the Bielefeld-Giessen Center for Microbial Bioinformatics (BiGi) of the German Federal Ministry of Education and Research-funded German network for bioinformatics infrastructure (de.NBI, grant 031A533) for providing computational resources and related general support. Sequence data are available here: PRJEB35573, ENA, EMBL-EBI and MN747968-78 (submission ID: 2287280, Genbank, NCBI).

Figure Legends

Fig. 1. Cadmium tolerance and accumulation in three populations of *A. halleri*. (a) Proportion of individuals maintaining root growth (elongation) as a function of Cd concentration. Dashed vertical lines indicate ED_{50}, the effective dose required to reach a proportion of 50% according to a dose-response model (see supplementary table 2, supplementary fig. 1, Supplementary Material online). (b) Cd tolerance index. Bars represent mean ± SD of EC_{100} (effective Cd concentration causing 100% root growth inhibition) in a given plant individual (Schat and Ten Bookum 1992). Plants were sequentially exposed to stepwise increasing concentrations of $CdSO_4$ in hydroponic culture every week (n = 6 to 9 per population, with one to three vegetative clones of each three to six genotypes per population; (a, b)). (c) Cd accumulation efficiency at the site of origin calculated from published field survey data (bars represent means ± SD of n = 11 to 12 individuals in the field; units employed, µg Cd g^{-1} dry biomass in leaves, µg total Cd g^{-1} dry mass in soil; data from Stein et al. 2017). (d) Cd concentration in root and shoot tissues of hydroponically cultivated plants. Shown are mean ± SD (n = 12 to 20 clones per population comprising both genotypes, from all three replicate experiments; see supplementary table 1, Supplementary Material online). Four-week-old vegetative clones were exposed to 0 (-Cd) and 2 µM $CdSO_4$ (+Cd) in hydroponic culture for 16 d alongside the plants cultivated for RNA-seq. Different characters denote statistically significant differences between means based on two-way ANOVA, followed by Tukey's HSD test (Log-transformed data were used

in (c)) ($P < 0.05$; see supplementary table 3, Supplementary Material online, for nested ANOVA of genotypes within a population (d)).

Fig. 2. Between-population differences according to transcriptome sequencing. (a, b) Venn diagrams show the numbers of genes exhibiting differential transcript abundances under exposure to Cd (+Cd) compared to control conditions (-Cd) for the three populations Noss (N), Pais (P) and Wall (W) in root (a) and shoot (b) tissues. Upregulation (red): Log_2(fold change +Cd *vs*. –Cd) = $Log_2FC > 0.5$; downregulation (blue): $Log_2FC < -0.5$; all with adjusted *P*-value < 0.05. (c, d) Venn diagrams show the numbers of genes exhibiting differential transcript abundance between populations in root (c) and shoot (d) tissues of plants cultivated under Cd exposure (violet) or control conditions (orange) ($|Log_2FC| > 0.5$; adjusted *P*-value < 0.05). Red lines surround genes differentially expressed between Noss and both populations of NM soils (Pais and Wall). Four-week-old vegetative clones were exposed to 2 µM Cd or 0 µM Cd (controls) in hydroponic culture for 16 d before harvest. Data are from three independent experiments (repeats), with two genotypes per population and material pooled from six replicate vegetative clones (three hydroponic culture vessels) per genotype in each experiment.

Fig. 3. Candidate genes differentially expressed in Noss compared to both other populations Pais and Wall. (a, b) Significantly enriched gene ontology (GO) categories for roots (a) and shoots (b) of plants cultivated in 0 µM Cd (see fig. 2c and d, Data Set 3). Genes differentially expressed between Noss from M soil and both Pais and Wall from NM soils were subjected to a GO term enrichment analysis. The number of genes in each over-represented category is shown inside bars (see Data Set 4 for all genes). (c, d) Relative transcript levels of the top three genes (largest between-population differences) taken from (a) and (b) in the over-represented GO category meiotic cell cycle, for roots (c) and shoots (d). (e-g) Relative transcript levels of metal homeostasis genes of which transcript levels are high (e, g) and low (f) in Noss (N) compared to both Pais (P) and Wall (W), for roots (e, f) and shoots (g) (top three genes from supplementary table 8, Supplementary Material online). Bars show means ± SD ($n = 6$) of normalized counts, which were additionally normalized per kilobase of gene length (NCPK). Different characters represent statistically significant groups based on two-way ANOVA, followed by Tukey's HSD test ($P < 0.05$, see supplementary table 6, Supplementary Material online, for details). Data are from the same experiment as shown in fig. 2. (h) Immunoblot detection of IRT1. Total protein extracts (40 µg) from roots of Noss_05 (N), Pais_09 (P) and Wall_07 (W) cultivated under control condition or exposed to 2 µM Cd as used in transcriptome sequencing, and total protein extract (10 µg) from roots of Fe- and Zn-deficient *A. thaliana* (*At*; positive control) were separated on a denaturing polyacrylamide gel, blotted, and detection was carried out using an anti-IRT1

antibody. Asterisks mark additional bands at positions that are consistent with *IRT1-Ub_2 (di-ubiquitinated form), **IRT1-Ub_3, ***IRT1-Ub_4, respectively. Coomassie Blue (CB) staining of the blotted membrane served as loading control.

Fig. 4. Functional classification of the transcriptional response to Cd. Significantly enriched GO categories among the transcriptional responses to Cd common in both the Pais and Wall populations for roots (a) and shoots (b) (see fig. 2a and b, Data Set 6). The numbers of genes in each over-represented category are shown inside bars. Data are from the same experiment as shown in fig. 2.

Fig. 5. Genome-wide sum of transcript levels contributed by different types of transposable elements in Noss, Pais and Wall. (a-d) Bars show means ± SD (n = 6) of transcript levels of transposable elements (TEs), corresponding to the sum total of RPKM for LTR (Long terminal repeat) retrotransposons (a, b) and non-LTR TEs (c, d) in root (a, c) and shoot (b, d), with RPKM ≥ 7 per locus. Different characters represent statistically significant differences based on one-way ANOVA, followed by Tukey's HSD test ($P < 0.05$).

Fig. 6. *ARGONAUTE 9* (*AGO9*) transcript levels in *A. halleri* individuals originating from metalliferous and non-metalliferous soils in Italy, Poland and Germany. Bargraph shows mean ± SD (n = 4) of relative *AGO9* transcript levels quantified by RT-qPCR in leaves of 5.5-week-old vegetative clones cultivated hydroponically (technical replicates, with two independent PCR runs on each of two independently synthesized cDNAs from a pool of six replicate clones). Data are shown relative to the constitutively expressed gene *Helicase* (*HEL*). Each PCR reaction was conducted in hexuplicate. Different characters represent statistically significant differences based on one-way ANOVA, followed by Tukey's HSD test ($P < 0.05$). For details on collection sites and individuals see Stein et al. 2017.

References

Arnold BJ, Lahner B, DaCosta JM, Weisman CM, Hollister JD, Salt DE, Bomblies K, Yant L. 2016. Borrowed alleles and convergence in serpentine adaptation. *Proc Natl Acad Sci USA* 113:8320-8325.

Baliardini C, Meyer CL, Salis P, Saumitou-Laprade P, Verbruggen N. 2015. CATION EXCHANGER1 cosegregates with cadmium tolerance in the metal hyperaccumulator *Arabidopsis halleri* and plays a role in limiting oxidative stress in *Arabidopsis* spp. *Plant Physiol* 169:549-559.

Barberon M, Zelazny E, Robert S, Conejero G, Curie C, Friml J, Vert G. 2011. Monoubiquitin-dependent endocytosis of the iron-regulated transporter 1 (IRT1) transporter controls iron uptake in plants. *Proc Natl Acad Sci USA* 108:E450-458.

Becher M, Talke IN, Krall L, Krämer U. 2004. Cross-species microarray transcript profiling reveals high constitutive expression of metal homeostasis genes in shoots of the zinc hyperaccumulator *Arabidopsis halleri*. *Plant J* 37:251-268.

Bert V, MacNair MR, De Laguérie P, Saumitou-Laprade P, Petit D. 2000. Zinc tolerance and accumualtion in metallicolous and non metallicolous populations of *Arabidopsis halleri* (Brassicaceae). *New Phytol* 146:225-233.

Bouyer D, Heese M, Chen P, Harashima H, Roudier F, Gruttner C, Schnittger A. 2018. Genome-wide identification of RETINOBLASTOMA RELATED 1 binding sites in Arabidopsis reveals novel DNA damage regulators. *PLoS Genet* 14:e1007797.

Briskine RV, Paape T, Shimizu-Inatsugi R, Nishiyama T, Akama S, Sese J, Shimizu KK. 2017. Genome assembly and annotation of *Arabidopsis halleri*, a model for heavy metal hyperaccumulation and evolutionary ecology. *Mol Ecol Resour* 17:1025-1036.

Cailliatte R, Schikora A, Briat JF, Mari S, Curie C. 2010. High-affinity manganese uptake by the metal transporter NRAMP1 is essential for Arabidopsis growth in low manganese conditions. *Plant Cell* 22:904-917.

Callis J. 2014. The ubiquitination machinery of the ubiquitin system. *Arabidopsis Book* 12:e0174.

Corso M, Schvartzman MS, Guzzo F, Souard F, Malkowski E, Hanikenne M, Verbruggen N. 2018. Contrasting cadmium resistance strategies in two metallicolous populations of *Arabidopsis halleri*. *New Phytol* 218:283-297.

de la Torre VSG, Majorel-Loulergue C, Gonzalez DA, Soubigou-Taconnat L, Rigaill GJ, Pillon Y, Barreau L, Thomine S, Fogliani B, Burtet-Sarramegna V, et al. 2018. Wide cross-species RNA-Seq comparison reveals a highly conserved role for Ferroportins in nickel hyperaccumulation in plants. *bioRxiv*:420729.

Deinlein U, Weber M, Schmidt H, Rensch S, Trampczynska A, Hansen TH, Husted S, Schjoerring JK, Talke IN, Krämer U, et al. 2012. Elevated nicotianamine levels in *Arabidopsis halleri* roots play a key role in zinc hyperaccumulation. *Plant Cell* 24:708-723.

Dräger DB, Desbrosses-Fonrouge AG, Krach C, Chardonnens AN, Meyer RC, Saumitou-Laprade P, Krämer U. 2004. Two genes encoding *Arabidopsis halleri* MTP1 metal transport proteins co-segregate with zinc tolerance and account for high *MTP1* transcript levels. *Plant J* 39:425-439.

Dubest S, Gallego ME, White CI. 2004. Roles of the AtERCC1 protein in recombination. *Plant J* 39:334-342.

Duran-Figueroa N, Vielle-Calzada JP. 2010. ARGONAUTE9-dependent silencing of transposable elements in pericentromeric regions of Arabidopsis. *Plant Signal Behav* 5:1476-1479.

Ernst WHO. 1974. Schwermetallvegetationen der Erde. Stuttgart, Germany: Gustav Fischer Verlag.

Fernandes JB, Duhamel M, Seguela-Arnaud M, Froger N, Girard C, Choinard S, Solier V, De Winne N, De Jaeger G, Gevaert K, et al. 2018. FIGL1 and its novel partner FLIP form a conserved complex that regulates homologous recombination. *PLoS Genet* 14:e1007317.

Geuting V, Kobbe D, Hartung F, Durr J, Focke M, Puchta H. 2009. Two distinct MUS81-EME1 complexes from Arabidopsis process Holliday junctions. *Plant Physiol* 150:1062-1071.

Grandbastien MA. 2015. LTR retrotransposons, handy hitchhikers of plant regulation and stress response. *Biochim Biophys Acta* 1849:403-416.

Halimaa P, Blande D, Baltzi E, Aarts MGM, Granlund L, Keinanen M, Karenlampi SO, Kozhevnikova AD, Peraniemi S, Schat H, et al. 2019. Transcriptional effects of cadmium on iron homeostasis differ in calamine accessions of *Noccaea caerulescens*. *Plant J* 97:306-320.

Hanikenne M, Talke IN, Haydon MJ, Lanz C, Nolte A, Motte P, Kroymann J, Weigel D, Krämer U. 2008. Evolution of metal hyperaccumulation required *cis*-regulatory changes and triplication of *HMA4*. *Nature* 453:391-395.

Hefner E, Preuss SB, Britt AB. 2003. Arabidopsis mutants sensitive to gamma radiation include the homologue of the human repair gene ERCC1. *J Exp Bot* 54:669-680.

Honjo MN, Kudoh H. 2019. *Arabidopsis halleri*: a perennial model system for studying population differentiation and local adaptation. *AoB PLANTS* 11.

Horvath V, Merenciano M, Gonzalez J. 2017. Revisiting the relationship between transposable elements and the eukaryotic stress response. *Trends Genet* 33:832-841.

Hussain D, Haydon MJ, Wang Y, Wong E, Sherson SM, Young J, Camakaris J, Harper JF, Cobbett CS. 2004. P-type ATPase heavy metal transporters with roles in essential zinc homeostasis in Arabidopsis. *Plant Cell* 16:1327-1339.

Kazemi-Dinan A, Thomaschky S, Stein RJ, Krämer U, Müller C. 2014. Zinc and cadmium hyperaccumulation act as deterrents towards specialist herbivores and impede the performance of a generalist herbivore. *New Phytol* 202:628-639.

Kerkeb L, Mukherjee I, Chatterjee I, Lahner B, Salt DE, Connolly EL. 2008. Iron-induced turnover of the Arabidopsis IRON-REGULATED TRANSPORTER1 metal transporter requires lysine residues. *Plant Physiol* 146:1964-1973.

Kim D, Langmead B, Salzberg SL. 2015. HISAT: a fast spliced aligner with low memory requirements. *Nat Methods* 12:357-360.

Kovalchuk O, Titov V, Hohn B, Kovalchuk I. 2001. A sensitive transgenic plant system to detect toxic inorganic compounds in the environment. *Nat Biotechnol* 19:568-572.

Krämer U. 2015. Planting molecular functions in an ecological context with *Arabidopsis thaliana*. *Elife* 4.

Krämer U. 2018. Conceptualizing plant systems evolution. *Curr Opin Plant Biol* 42:66-75.

Lamas GA, Navas-Acien A, Mark DB, Lee KL. 2016. Heavy Metals, Cardiovascular Disease, and the Unexpected Benefits of Chelation Therapy. *J Am Coll Cardiol* 67:2411-2418.

Lämmli UK. 1970. Cleavage of structural proteins during the assembly of the head of bacteriophage T4. *Nature* 227:680-685.

Leskova A, Giehl RFH, Hartmann A, Fargasova A, von Wiren N. 2017. Heavy Metals Induce Iron Deficiency Responses at Different Hierarchic and Regulatory Levels. *Plant Physiol* 174:1648-1668.

Liu M, Ba Z, Costa-Nunes P, Wei W, Li L, Kong F, Li Y, Chai J, Pontes O, Qi Y. 2017. IDN2 Interacts with RPA and Facilitates DNA Double-Strand Break Repair by Homologous Recombination in Arabidopsis. *Plant Cell* 29:589-599.

Love MI, Huber W, Anders S. 2014. Moderated estimation of fold change and dispersion for RNA-seq data with DESeq2. *Genome Biol* 15:550.

Meier SK, Adams N, Wolf M, Balkwill K, Muasya AM, Gehring CA, Bishop JM, Ingle RA. 2018. Comparative RNA-seq analysis of nickel hyperaccumulating and non-accumulating populations of *Senecio coronatus* (Asteraceae). *Plant J* 95:1023-1038.

Mercier R, Mezard C, Jenczewski E, Macaisne N, Grelon M. 2015. The molecular biology of meiosis in plants. *Annu Rev Plant Biol* 66:297-327.

Meyer CL, Juraniec M, Huguet S, Chaves-Rodriguez E, Salis P, Isaure MP, Goormaghtigh E, Verbruggen N. 2015. Intraspecific variability of cadmium tolerance and accumulation, and cadmium-induced cell wall modifications in the metal hyperaccumulator *Arabidopsis halleri*. *J Exp Bot* 66:3215-3227.

Meyer CL, Vitalis R, Saumitou-Laprade P, Castric V. 2009. Genomic pattern of adaptive divergence in *Arabidopsis halleri*, a model species for tolerance to heavy metal. *Mol Ecol* 18:2050-2062.

Morales ME, Derbes RS, Ade CM, Ortego JC, Stark J, Deininger PL, Roy-Engel AM. 2016. Heavy metal exposure influences double strand break DNA repair outcomes. *PLoS One* 11:e0151367.

Mortazavi A, Williams BA, McCue K, Schaeffer L, Wold B. 2008. Mapping and quantifying mammalian transcriptomes by RNA-Seq. *Nat Methods* 5:621-628.

Nagano AJ, Kawagoe T, Sugisaka J, Honjo MN, Iwayama K, Kudoh H. 2019. Annual transcriptome dynamics in natural environments reveals plant seasonal adaptation. *Nat Plants* 5:74-83.

Nriagu JO, Pacyna JM. 1988. Quantitative assessment of worldwide contamination of air, water and soils by trace metals. *Nature* 333:134-139.

Okonechnikov K, Conesa A, Garcia-Alcalde F. 2016. Qualimap 2: advanced multi-sample quality control for high-throughput sequencing data. *Bioinformatics* 32:292-294.

Oliver C, Santos JL, Pradillo M. 2014. On the role of some ARGONAUTE proteins in meiosis and DNA repair in *Arabidopsis thaliana*. *Front Plant Sci* 5:177.

Olmedo-Monfil V, Duran-Figueroa N, Arteaga-Vazquez M, Demesa-Arevalo E, Autran D, Grimanelli D, Slotkin RK, Martienssen RA, Vielle-Calzada JP. 2010. Control of female gamete formation by a small RNA pathway in Arabidopsis. *Nature* 464:628-632.

Pauwels M, Saumitou-Laprade P, Holl AC, Petit D, Bonnin I. 2005. Multiple origin of metallicolous populations of the pseudometallophyte *Arabidopsis halleri* (Brassicaceae) in central Europe: the cpDNA testimony. *Mol Ecol* 14:4403-4414.

Pauwels M, Vekemans X, Gode C, Frerot H, Castric V, Saumitou-Laprade P. 2012. Nuclear and chloroplast DNA phylogeography reveals vicariance among European populations of the model species for the study of metal tolerance, *Arabidopsis halleri* (Brassicaceae). *New Phytol* 193:916-928.

Pietzenuk B, Markus C, Gaubert H, Bagwan N, Merotto A, Bucher E, Pecinka A. 2016. Recurrent evolution of heat-responsiveness in Brassicaceae COPIA elements. *Genome Biol* 17:209.

Preite V, Sailer C, Syllwasschy L, Bray S, Ahmadi H, Kramer U, Yant L. 2019. Convergent evolution in *Arabidopsis halleri* and *Arabidopsis arenosa* on calamine metalliferous soils. *Philos Trans R Soc Lond B Biol Sci* 374:20180243.

R: A language and environment for statistical computing [Internet]. Vienna, Austria: Foundation for Statistical Computing; 2013. Available from: http://www.R-project.org/

Reeves RD, Baker AJM, Jaffre T, Erskine PD, Echevarria G, van der Ent A. 2018. A global database for plants that hyperaccumulate metal and metalloid trace elements. *New Phytol* 218:407-411.

Reimand J, Arak T, Adler P, Kolberg L, Reisberg S, Peterson H, Vilo J. 2016. g:Profiler-a web server for functional interpretation of gene lists (2016 update). *Nucleic Acids Res* 44:W83-89.

Robinson JT, Thorvaldsdottir H, Wenger AM, Zehir A, Mesirov JP. 2017. Variant Review with the Integrative Genomics Viewer. *Cancer Res* 77:e31-e34.

Rounds MA, Larsen PB. 2008. Aluminum-dependent root-growth inhibition in Arabidopsis results from AtATR-regulated cell-cycle arrest. *Curr Biol* 18:1495-1500.

Sakamoto T, Inui YT, Uraguchi S, Yoshizumi T, Matsunaga S, Mastui M, Umeda M, Fukui K, Fujiwara T. 2011. Condensin II alleviates DNA damage and is essential for tolerance of boron overload stress in Arabidopsis. *Plant Cell* 23:3533-3546.

Schat H, Ten Bookum WM. 1992. Genetic control of copper tolerance in *Silene vulgaris*. *Heredity* 68:219-229.

Schuermann D, Molinier J, Fritsch O, Hohn B. 2005. The dual nature of homologous recombination in plants. *Trends Genet* 21:172-181.

Schvartzman MS, Corso M, Fataftah N, Scheepers M, Nouet C, Bosman B, Carnol M, Motte P, Verbruggen N, Hanikenne M. 2018. Adaptation to high zinc depends on distinct mechanisms in metallicolous populations of *Arabidopsis halleri*. *New Phytol* 218:269-282.

Seeliger K, Dukowic-Schulze S, Wurz-Wildersinn R, Pacher M, Puchta H. 2012. BRCA2 is a mediator of RAD51- and DMC1-facilitated homologous recombination in *Arabidopsis thaliana*. *New Phytol* 193:364-375.

Sinclair SA, Senger T, Talke IN, Cobbett CS, Haydon MJ, Kramer U. 2018. Systemic upregulation of MTP2- and HMA2-mediated Zn partitioning to the shoot supplements local Zn deficiency responses. *Plant Cell* 30:2463-2479.

Spampinato CP. 2017. Protecting DNA from errors and damage: an overview of DNA repair mechanisms in plants compared to mammals. *Cell Mol Life Sci* 74:1693-1709.

Stein RJ, Höreth S, de Melo JR, Syllwasschy L, Lee G, Garbin ML, Clemens S, Krämer U. 2017. Relationships between soil and leaf mineral composition are element-specific, environment-dependent and geographically structured in the emerging model *Arabidopsis halleri*. *New Phytol* 213:1274-1286.

Talke IN, Hanikenne M, Krämer U. 2006. Zinc-dependent global transcriptional control, transcriptional deregulation, and higher gene copy number for genes in metal homeostasis of the hyperaccumulator *Arabidopsis halleri*. *Plant Physiol* 142:148-167.

Turner TL, Bourne EC, Von Wettberg EJ, Hu TT, Nuzhdin SV. 2010. Population resequencing reveals local adaptation of *Arabidopsis lyrata* to serpentine soils. *Nat Genet* 42:260-263.

van der Pas L, Ingle RA. 2019. Towards an understanding of the molecular basis of nickel hyperaccumulation in plants. *Plants* 8:11.

Vaucheret H. 2008. Plant ARGONAUTES. *Trends Plant Sci* 13:350-358.

Vert G, Grotz N, Dedaldechamp F, Gaymard F, Guerinot ML, Briat JF, Curie C. 2002. IRT1, an Arabidopsis transporter essential for iron uptake from the soil and for plant growth. *Plant Cell* 14:1223-1233.

Weber M, Harada E, Vess C, Roepenack-Lahaye EV, Clemens S. 2004. Comparative microarray analysis of *Arabidopsis thaliana* and *Arabidopsis halleri* roots identifies nicotianamine synthase, a ZIP transporter and other genes as potential metal hyperaccumulation factors. *Plant J* 37:269-281.

Weber M, Trampczynska A, Clemens S. 2006. Comparative transcriptome analysis of toxic metal responses in *Arabidopsis thaliana* and the Cd(2+)-hypertolerant facultative metallophyte *Arabidopsis halleri*. *Plant Cell Environ* 29:950-963.

Yant L, Hollister JD, Wright KM, Arnold BJ, Higgins JD, Franklin FC, Bomblies K. 2013. Meiotic adaptation to genome duplication in *Arabidopsis arenosa*. *Curr Biol* 23:2151-2156.

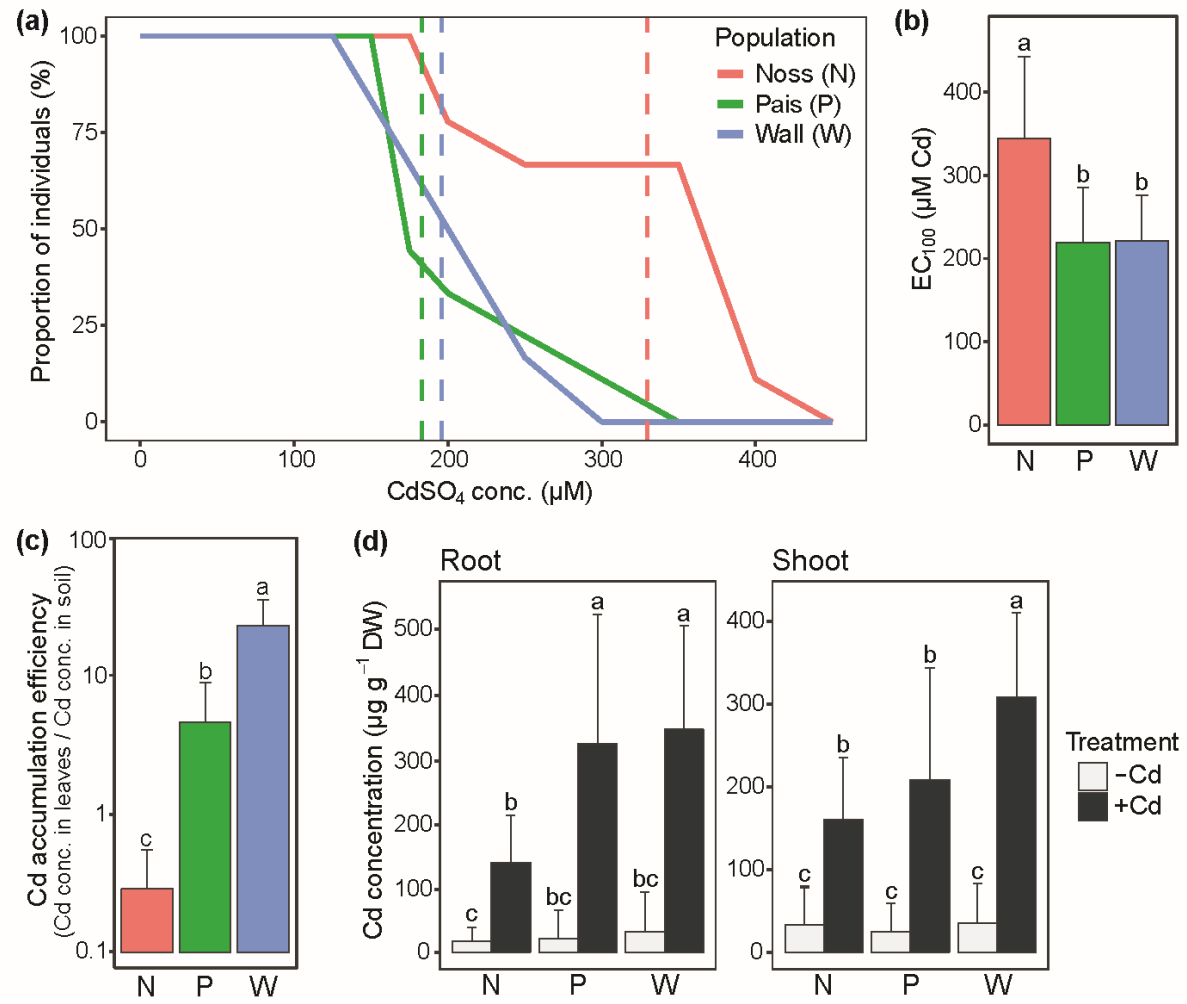

Fig. 1. Cadmium tolerance and accumulation in three populations of *A. halleri*. (a) Proportion of individuals maintaining root growth (elongation) as a function of Cd concentration. Dashed vertical lines indicate ED_{50}, the effective dose required to reach a proportion of 50% according to a dose-response model (see supplementary table 2, supplementary fig. 1, Supplementary Material online). (b) Cd tolerance index. Bars represent mean ± SD of EC_{100} (effective Cd concentration causing 100% root growth inhibition) in a given plant individual (Schat and Ten Bookum 1992). Plants were sequentially exposed to stepwise increasing concentrations of $CdSO_4$ in hydroponic culture every week (n = 6 to 9 per population, with one to three vegetative clones of each three to six genotypes per population; (a, b)). (c) Cd accumulation efficiency at the site of origin calculated from published field survey data (bars represent means ± SD of n = 11 to 12 individuals in the field; units employed, μg Cd g^{-1} dry biomass in leaves, μg total Cd g^{-1} dry mass in soil; data from Stein, et al. 2017). (d) Cd concentration in root and shoot tissues of hydroponically cultivated plants. Shown are mean ± SD (n = 12 to 20 clones per population comprising both genotypes, from all three replicate experiments; see supplementary table 1, Supplementary Material online). Four-week-old vegetative clones were exposed to 0 (-Cd) and 2 μM $CdSO_4$ (+Cd) in hydroponic culture for 16 d alongside the plants cultivated for RNA-seq. Different characters denote statistically significant differences between means based on two-way ANOVA, followed by Tukey's HSD test (Log-transformed data were used in (c)) (P < 0.05; see supplementary table 3, Supplementary Material online, for nested ANOVA of genotypes within a population (d)).

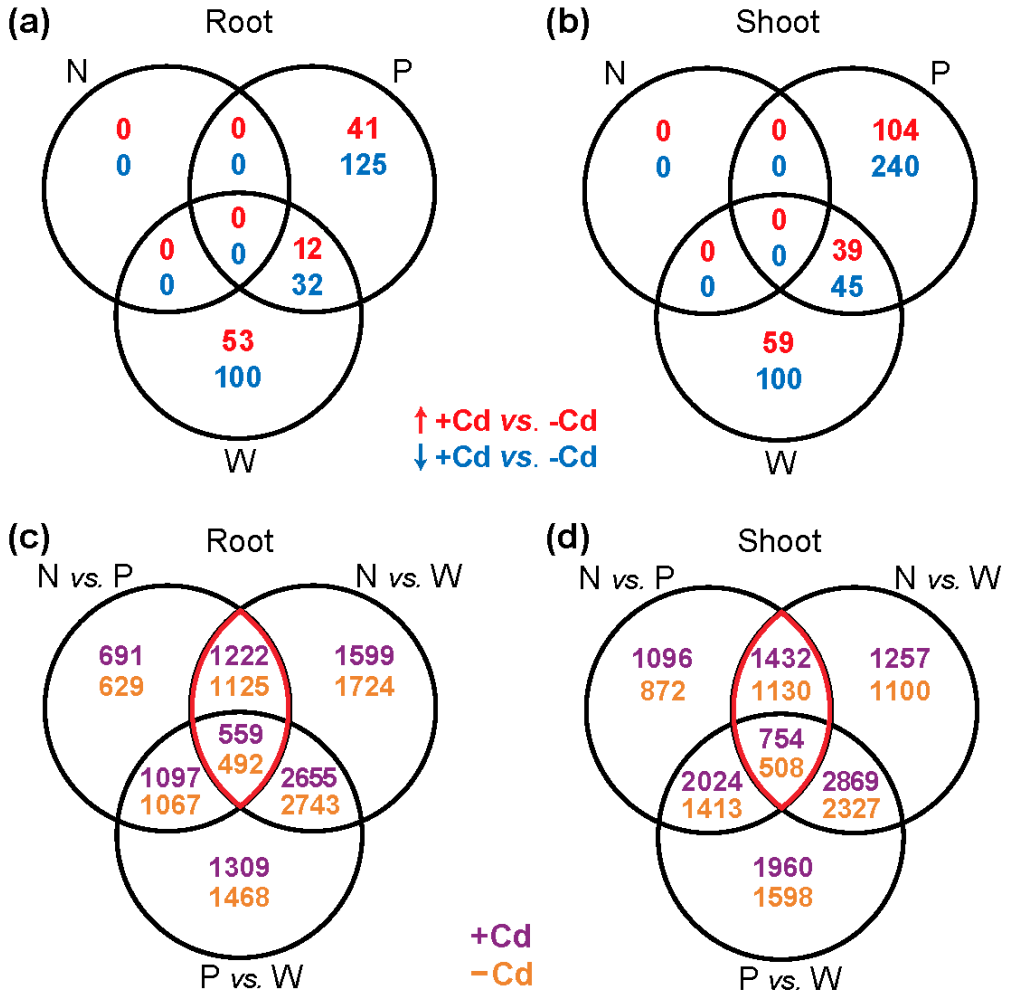

Fig. 2. Between-population differences according to transcriptome sequencing. (a, b) Venn diagrams show the numbers of genes exhibiting differential transcript abundances under exposure to Cd (+Cd) compared to control conditions (-Cd) for the three populations Noss (N), Pais (P) and Wall (W) in root (a) and shoot (b) tissues. Upregulation (red): Log_2(fold change +Cd *vs.* –Cd) = $Log_2FC > 0.5$; downregulation (blue): $Log_2FC < -0.5$; all with adjusted *P*-value < 0.05. (c, d) Venn diagrams show the numbers of genes exhibiting differential transcript abundance between populations in root (c) and shoot (d) tissues of plants cultivated under Cd exposure (violet) or control conditions (orange) ($|Log_2FC| > 0.5$; adjusted *P*-value < 0.05). Red lines surround genes differentially expressed between Noss and both populations of NM soils (Pais and Wall). Four-week-old vegetative clones were exposed to 2 µM Cd or 0 µM Cd (controls) in hydroponic culture for 16 d before harvest. Data are from three independent experiments (repeats), with two genotypes per population and material pooled from six replicate vegetative clones (three hydroponic culture vessels) per genotype in each experiment.

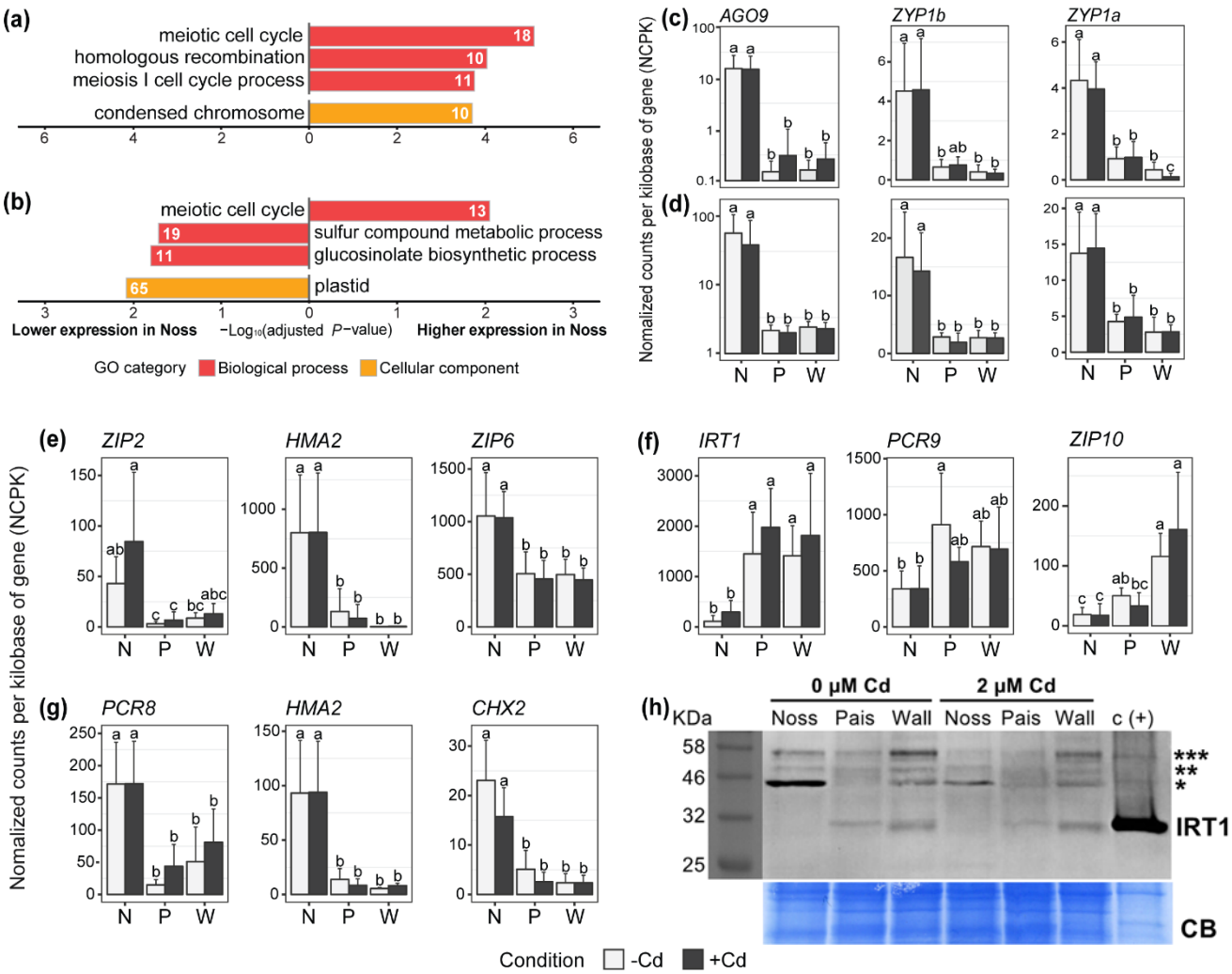

Fig. 3. Candidate genes differentially expressed in Noss compared to both other populations Pais and Wall. (a, b) Significantly enriched gene ontology (GO) categories for roots (a) and shoots (b) of plants cultivated in 0 µM Cd (see fig. 2c and d, Data Set 3). Genes differentially expressed between Noss from M soil and both Pais and Wall from NM soils were subjected to a GO term enrichment analysis. The number of genes in each over-represented category is shown inside bars (see Dataset S4 for all genes). (c, d) Relative transcript levels of the top three genes (largest between-population differences) taken from (a) and (b) in the over-represented GO category meiotic cell cycle, for roots (c) and shoots (d). (e-g) Relative transcript levels of metal homeostasis genes of which transcript levels are high (e, g) and low (f) in Noss (N) compared to both Pais (P) and Wall (W), for roots (e, f) and shoots (g) (top three genes from supplementary table 8, Supplementary Material online). Bars show means ± SD (n = 6) of normalized counts, which were additionally normalized per kilobase of gene length (NCPK). Different characters represent statistically significant groups based on two-way ANOVA, followed by Tukey's HSD test (P < 0.05, see supplementary table 6, Supplementary Material online, for details). Data are from the same experiment as shown in fig. 2. (h) Immunoblot detection of IRT1. Total protein extracts (40 µg) from roots of Noss_05 (N), Pais_09 (P) and Wall_07 (W) cultivated under control condition or exposed to 2 µM Cd as used in transcriptome sequencing, and total protein extract (10 µg) from roots of Fe- and Zn-deficient *A. thaliana* (*At*; positive control) were separated on a denaturing polyacrylamide gel, blotted, and detection was carried out using an anti-IRT1 antibody. Asterisks mark additional bands at positions that are consistent with *IRT1-Ub_2 (di-ubiquitinated form), **IRT1-Ub_3, ***IRT1-Ub_4, respectively. Coomassie Blue (CB) staining of the blotted membrane served as loading control.

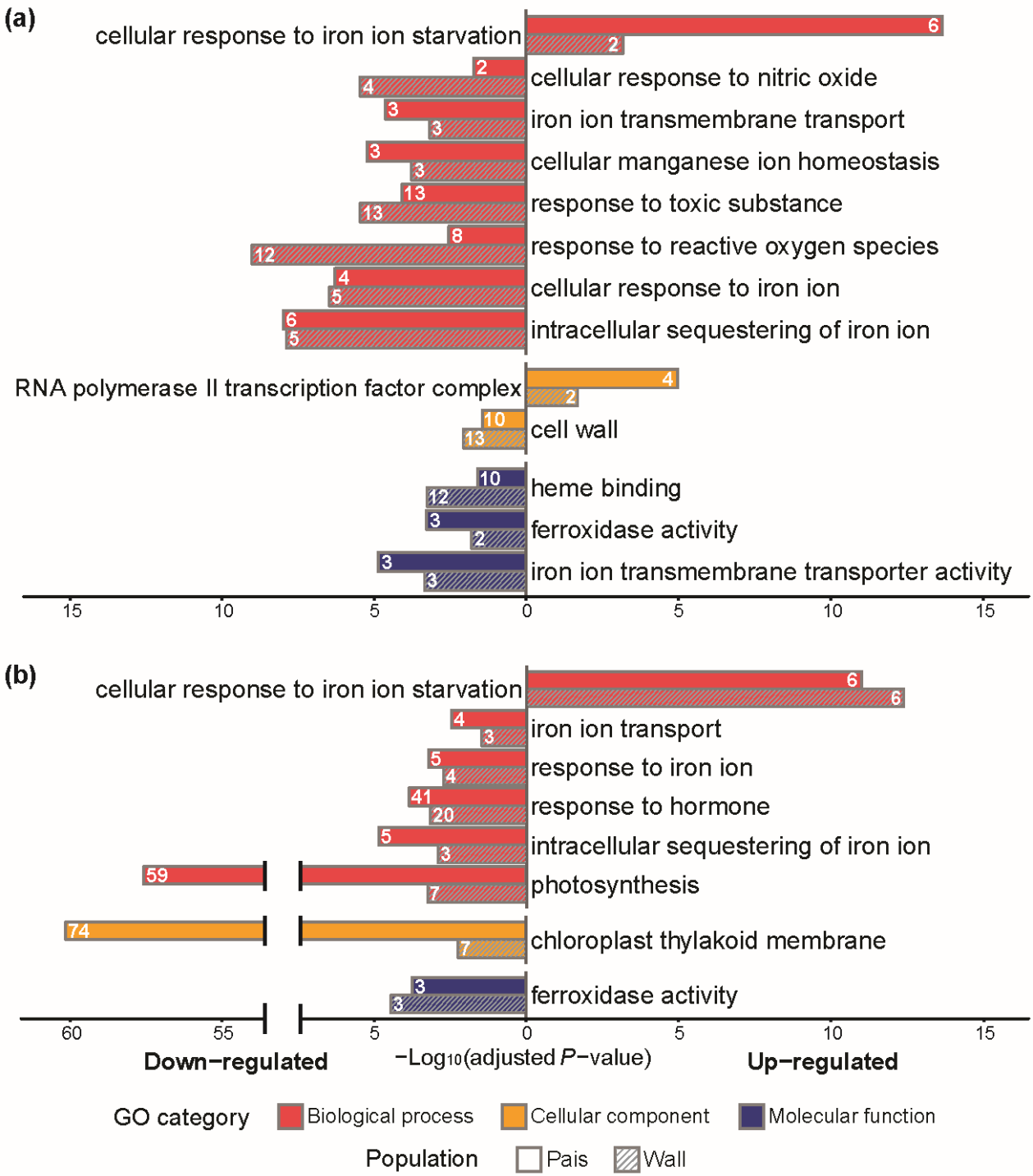

Fig. 4. Functional classification of the transcriptional response to Cd. Significantly enriched GO categories among the transcriptional responses to Cd common in both the Pais and Wall populations for roots (a) and shoots (b) (see fig. 2a and b, Data Set 6). The numbers of genes in each over-represented category are shown inside bars. Data are from the same experiment as shown in fig. 2.

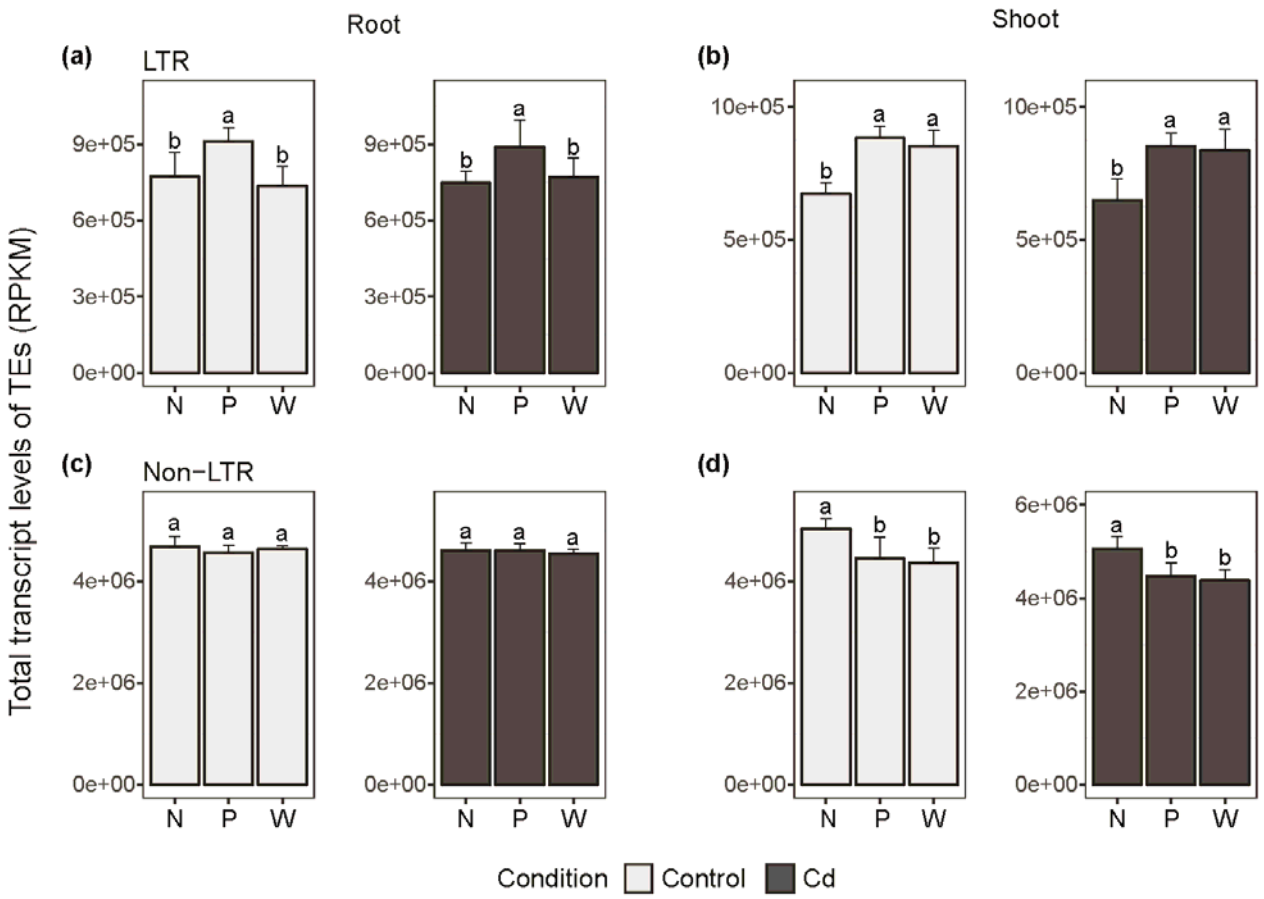

Fig. 5. Genome-wide sum of transcript levels contributed by different types of transposable elements in Noss, Pais and Wall. (a-d) Bars show means ± SD (n = 6) of transcript levels of transposable elements (TEs), corresponding to the sum total of RPKM for LTR (Long terminal repeat) retrotransposons (a, b) and non-LTR TEs (c, d) in root (a, c) and shoot (b, d), with RPKM $\geq$ 7 per locus. Different characters represent statistically significant differences based on one-way ANOVA, followed by Tukey's HSD test ($P < 0.05$).

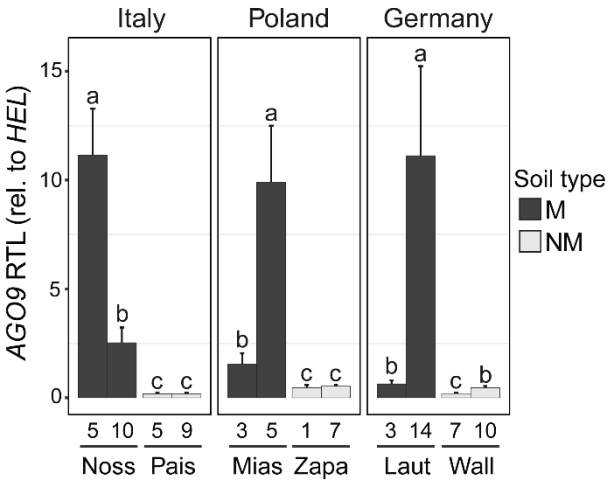

Fig. 6. *ARGONAUTE9* (*AGO9*) transcript levels in *A. halleri* individuals originating from metalliferous and non-metalliferous soils in Italy, Poland and Germany. Bargraph shows mean ± SD (n = 4) of relative *AGO9* transcript levels quantified by RT-qPCR in leaves of 5.5-week-old vegetative clones cultivated hydroponically (technical replicates, with two independent PCR runs on each of two independently synthesized cDNAs from a pool of six replicate clones). Data are shown relative to the constitutively expressed gene *Helicase* (*HEL*). Each PCR reaction was conducted in hexuplicate. Different characters represent statistically significant differences based on one-way ANOVA, followed by Tukey's HSD test ($P < 0.05$). For details on collection sites and individuals see Stein, et al. 2017.